

## ORTHO-PARA HYDROGEN CONVERSION CATALYZED BY GOLD NANOPARTICLES

ABKHALIMOV Evgeny<sup>1</sup>, BOEVA Ol'ga<sup>2</sup>, ODINTZOV Alexandr<sup>2</sup>, SOLOVOV Roman<sup>1</sup>,  
ZHAVORONKOVA Ksenia<sup>2</sup>, ERSHOV Boris<sup>1</sup>

<sup>1</sup>A.N. Frumkin Institute of Physical Chemistry and Electrochemistry, Russian Academy of Science, Moscow, Russian Federation

<sup>2</sup>Mendeleev University of Chemical Technology of Russia, Moscow, Russian Federation

### Abstract

We set ourselves the task to perform a systematic study of the *ortho-para* conversion of protium catalyzed by  $\gamma$ -Al<sub>2</sub>O<sub>3</sub>-supported gold nanoparticles of various sizes at a temperature of 77 K. Our results unambiguously indicate that nanoparticles, as opposed to the bulk metal, shown a high catalytic activity. It is exhibited that all Au/ $\gamma$ -Al<sub>2</sub>O<sub>3</sub> catalysts with nanoparticles of 4.6-40.1 nm sizes show very high catalytic activity in *ortho-para* conversion reaction. The calculated specific catalytic activity  $K_{sp}$  of *ortho-para* hydrogen conversion were  $(3.9 \pm 1.2) \times 10^{14}$  mol cm<sup>-2</sup>·s<sup>-1</sup> for all of the catalysts tested. The conversion of *o*-protium to *p*-protium catalyzed by gold nanoparticles does not depend on the nanoparticle size.

**Keywords:** Gold nanoparticles, protium, *ortho-para* conversion, size effect, hydrogen

### 1. INTRODUCTION

Gold nanoparticles, unlike the bulk metal, are able to catalyze many organic reactions. This is characteristic of particles supported on various materials [1-4] and particles in an aqueous solution [5-7]. It was shown that the smaller the particle size, the higher the specific catalytic activity. The highest efficiency was found for gold particles of  $3 \leq d \leq 5$  nm size [8-10]. As the particle size increases, the catalytic activity considerably decreases. For reactions involving molecular hydrogen, this size dependence of the catalytic activity is attributed to the structural state of the particle surface. Presumably, a decrease in the particle size is accompanied by relative increase in the number of low-coordination faces and corners [3, 11]. Large number of low-coordinated atoms in small particles leads to activation and dissociation of hydrogen molecules on the gold surface. There is a certain correlation between the catalytic activity of gold nanoparticles of various size and the number of low-coordination faces and corners [5, 10].

Previously, we found [12] that gold nanoparticles supported on  $\gamma$ -Al<sub>2</sub>O<sub>3</sub> show catalytic activity in the homomolecular hydrogen isotope exchange  $H_2 + D_2 \leftrightarrow 2HD$ . The most pronounced difference between the catalytic properties of particles is observed at low temperature (77 K). The specific rate of the catalytic reaction on smaller particles (4.6 nm) is about 20 times as high as that on larger particles (19.4 nm). It was also shown that gold nanoparticles catalyze the *ortho* (*o*)-to-*para* (*p*) hydrogen conversion. The reaction rate is almost two orders of magnitude higher than the isotope exchange rate. Preliminary experiments showed unexpectedly that the specific reaction rate does not depend on the nanoparticle size. These results indicate that the *ortho-para* hydrogen conversion catalyzed by gold nanoparticles follows a different mechanism not inherent in organic synthesis reactions involving hydrogen.

The *ortho-para* conversion of hydrogen is the transition of *ortho*-protium (nuclear spins of atoms in the molecule point in the same direction) to the *para*-protium (nuclear spins point to the opposite directions). The reaction involves two hydrogen molecules, *i.e.*, it is bimolecular. Unlike the liquid phase in which the *ortho-para* conversion is spontaneous, in the gas phase, this reaction barely proceeds, which is caused by very weak interaction between the *o*-H<sub>2</sub> and *p*-H<sub>2</sub> molecules. In contrast to the gas phase, *o-p* conversion is promoted on

various solid surfaces [13, 14] by, in particular, silver [15-19], copper [20, 21], graphite [22, 23], and supported chromium and ferric oxides [24-27].

The spin conversion mechanism has been considered by B. F. Minaev *et al.* [28] and G. Buntkowsky *et al.* [29]. The *o-p* H<sub>2</sub> conversion is considerably promoted in the presence of magnetic materials and is induced by the magnetic dipole interaction and Fermi contact interaction [30-32]. The mechanism of *o-p* H<sub>2</sub> conversion on nonmagnetic metal surfaces has been attributed to the Coulomb-contact model [14, 17]. Recent progress of experimental and theoretical studies on the physisorption and *ortho-para* conversion of molecular hydrogen is discussed in a review by K. Fukutani *et al.* [13].

The *ortho-para* conversion of protium in hydrogen gas can be considered as a model reaction for studying the mechanisms of interactions of molecular hydrogen with the catalyst surface. This process is important for the low-temperature distillation technique for hydrogen isotope separation and for liquefaction and storage of liquid hydrogen. Previously, *ortho-para* hydrogen conversion catalyzed by metal nanoparticle-based systems has been scarcely studied.

We set ourselves the task to perform a systematic study of the *ortho-para* conversion of protium catalyzed by  $\gamma$ -Al<sub>2</sub>O<sub>3</sub>-supported gold nanoparticles of various sizes (from 4.6 nm to 40.1 nm) at a temperature of 77 K. Our results unambiguously indicate that nanoparticles, as opposed to the bulk metal, exhibit a high catalytic activity. However, the specific rate of this reaction, unlike that of organic reactions involving molecular hydrogen, virtually does not depend on the particle size.

## 2. EXPERIMENTAL

Gold nanoparticles were obtained by reducing AuCl<sub>4</sub><sup>-</sup> ions with citrate ions in aqueous solutions with heating according to the Turkevich procedure [33]; on exposure to pulsed UV radiation [5, 34]; combined reduction with citrate ions and hydrogen [5]; and reduction with tannin [36]. The syntheses were monitored by spectrophotometry by observing the optical absorption of the surface plasmons of gold nanoparticles at 510-540 nm.

The nanoparticle size and shape were determined by transmission electron microscopy (TEM) on JEOL JEM-2100 instruments. Using the described methods, gold hydrosols with the following particle size were obtained and characterized: 4.6 ± 0.8, 7.4 ± 1.1, 14.4 ± 2.2, 19.4 ± 4.2, 20.5 ± 4.5, 28.1 ± 0.5, and 40.1 ± 5.4 nm. Gold nanoparticles were mainly spherically shaped and have unimodal size distribution.

The catalyst was obtained by depositing gold nanoparticles on  $\gamma$ -Al<sub>2</sub>O<sub>3</sub> from an aqueous solution. For this purpose, 1 g of  $\gamma$ -Al<sub>2</sub>O<sub>3</sub> was added with stirring to 5 ml of a solution of colloid gold and kept for 24 h. According to spectrophotometric data, almost the whole amount of the metal (more than 95 %) was attached to the support. Then alumina with supported gold was calcined at 573 K in air for 3 h and then heated in a vacuum to decompose organic compounds and attach the particles to the support.

The specific surface area of the catalysts was determined by measuring the low-temperature hydrogen adsorption (77 K) in the pressure range from 0.01 to 0.2 Torr until the monolayer coverage was formed.

The kinetics of *ortho-para* conversion of protium was studied under static conditions at a working pressure of 0.5 Torr and a temperature of 77 K. The gas mixture composition was measured continuously by a method based on different rotational heat capacity of *o*-H<sub>2</sub> and *p*-H<sub>2</sub> at low temperature. This was done using a classical modified two-cell system [36]. The working cell was a part of the reaction volume, while the reference cell was filled with the mixture of the starting composition. The cells had equal volumes and were maintained under identical conditions, being incorporated in a Wheatstone bridge circuit. Copper coils located close to each other in the circuit, preventing the temperature drift during operation, served for stabilization of the microvoltmeter readings.

### 3. RESULTS AND DISCUSSION

It was found that the *ortho-para* hydrogen conversion does not take place on the support without gold nanoparticles and also that it does not occur on bulk gold. Thus, hydrogen conversion is activated by nanoparticle deposition.

The rate of *ortho*-hydrogen conversion to *para*-hydrogen during the *ortho-para* conversion reaction is written as

$$-d[o-H_2]/dt = k[o-H_2] \quad (1)$$

This reaction gives *para*-hydrogen, the concentration of which will be designated by  $[p-H_2]$ . The initial *o*-H<sub>2</sub> concentration is  $[o-H_2]_0$  and, hence, the current concentration  $[o-H_2]_t = [o-H_2]_0 - [o-H_2]_x$ , where  $[o-H_2]_x$  is the concentration of *o*-H<sub>2</sub> that reacted and, hence, of *p*-H<sub>2</sub> that formed. Then, the kinetic equation for the first-order reaction and the solution has the following form:

$$d[p-H_2]/dt = k([o-H_2]_0 - [o-H_2]_x) \quad (2)$$

$$[p-H_2]_t = [o-H_2]_0(1 - e^{-kt}) \quad (3)$$

For the boundary conditions: when  $t = 0$ , then  $[p-H_2] = 0$ ; when  $t \rightarrow \infty$ , then  $[p-H_2] \rightarrow [p-H_2]_\infty$ .

The degree of *ortho-para* hydrogen conversion  $F$  is given by

$$F = [p-H_2]_t/[p-H_2]_\infty = n_t/n_\infty = 1 - e^{-kt} \quad (4)$$

where  $n_t$  is the signal (in relative units) proportional to the *p*-H<sub>2</sub> concentration at time point  $t$ ,  $n_\infty$  is the signal in the same units after a time sufficient for the equilibrium to be established.

$$\ln(1-F) = -kt \quad (5)$$

where  $k$  is the reaction rate constant measured experimentally.

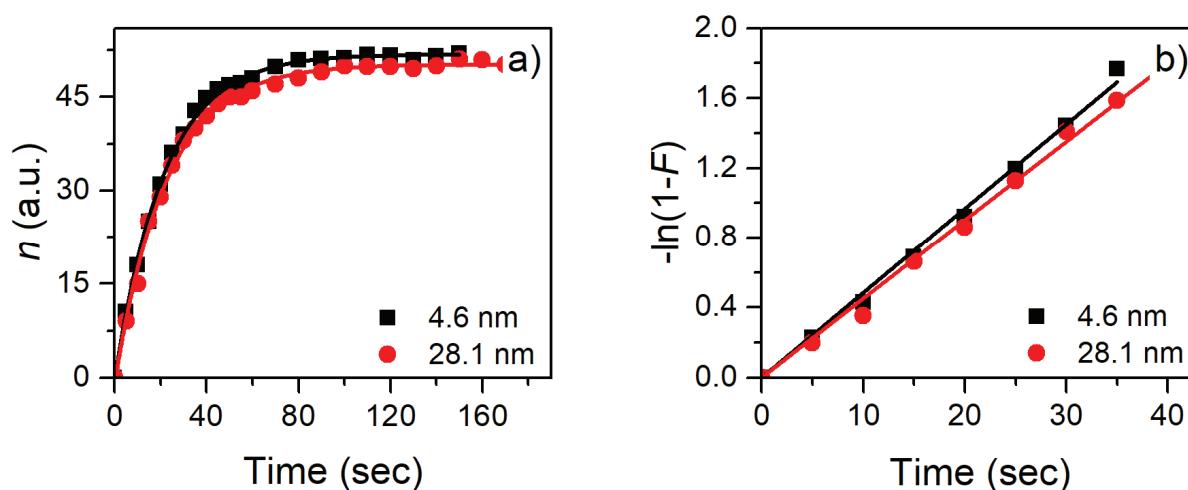


**Figure 1** Experimental kinetic curves for *o-p* hydrogen conversion (a) and graphical determination of the rate constants (b) for catalysts containing 4.6 and 28.1 nm gold nanoparticles

Using experimental data, kinetic curves were constructed (**Figure 1a**) and then the degrees of exchange  $F$  were determined from the curves. The rate constants for the first-order reaction  $k_0$  (**Figure 1b**) were calculated from the slope of the straight line plotted in the  $-\ln(1-F) - f(\tau)$  coordinates. The data of **Figure 1** clearly demonstrate that the kinetic dependences for the *ortho-para* hydrogen conversion obtained for catalysts

containing 4.6 nm and 28.1 nm nanoparticles virtually coincide. That is, the process is almost independent of the gold particle size.

The specific catalytic activity  $K_{sp}$  is defined as the first-order rate constant  $k_0$  divided by the catalyst active surface area  $S_H$  with allowance for the number of hydrogen atoms present in the reaction volume at the given temperature  $N_T$ . The  $N_T$  value is determined from the preliminary calibration of the reaction volume. Thus,

$$K_{sp} = k_0 N_T / S_H \text{ [molecule / (cm}^2 \cdot \text{s)]} \quad (6)$$

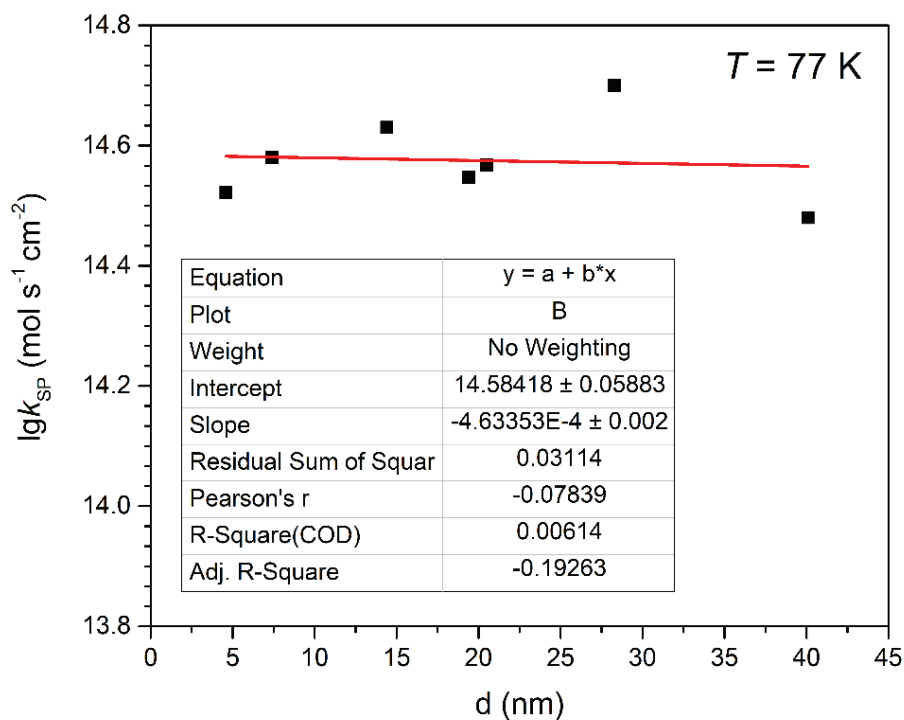


**Figure 2** Size dependence of the specific catalytic activity of gold nanoparticles in *ortho-para* hydrogen conversion at 77 K

The results of experiments showed that, as was to be expected, the  $S_H$  value decreases with increasing gold particle size. This trend is quite clear-cut. Indeed, for the catalyst containing gold particles of 4.6 nm size, the  $S_H$  value is  $0.11 \text{ m}^2 / \text{g}$ , while that for 40.1 nm particles is  $0.08 \text{ m}^2 / \text{g}$ . It was found that all catalyst samples with gold nanoparticles of 4.6, 7.4, 14.4, 19.4, 20.5, 28.1, and 40.1 nm sizes exhibited very high catalytic activity. The specific catalytic activity  $K_{sp}$  of *ortho-para* hydrogen conversion was  $(3.9 \pm 1.2) \times 10^{14}$  molecules /  $(\text{cm}^2 \cdot \text{s})$  for all of the gold nanoparticles tested. In other words, the conversion of *ortho*-protium (with nuclear spins of atoms in the molecule pointing in the same direction) to *para*-protium (with nuclear spins pointing in the opposite directions) catalyzed by gold nanoparticles does not depend on the nanoparticle size (**Figure 2**). This implies that the *ortho-para* hydrogen conversion follows a mechanism different from that of  $\text{H}_2\text{-D}_2$  exchange where the specific catalytic activity has a clear-cut dependence on the particle size [13].

The catalytic activity of gold nanoparticles of various sizes towards the *ortho-para* hydrogen conversion ( $3.9 \times 10^{14}$  molecules /  $(\text{cm}^2 \cdot \text{s})$ ) is much higher than that towards  $\text{H}_2\text{-D}_2$  exchange. Indeed, for 4.6 nm and 19.4 nm particles, the  $K_{sp}$  values for isotope exchange were  $1.4 \times 10^{13}$  and  $6.3 \times 10^{11}$  molecules /  $(\text{cm}^2 \cdot \text{s})$ , respectively [13]. That is, the  $K_{sp}$  values for the *ortho-para* conversion at 77 K are approximately 30 (for 4.6 nm) and even 600 (for 19.4 nm) times as high as those for  $\text{H}_2\text{-D}_2$  exchange reactions. This difference cannot be attributed to the kinetic isotope effect (in this case, the difference would be 2-4 times). It is evident that the isotope exchange and *ortho-para* conversion reactions follow different mechanisms. The mechanism of  $\text{H}_2\text{-D}_2$  exchange is chemical and involves dissociative absorption of hydrogen [12]. The *ortho-para*

conversion of protium is apparently promoted by the specific state of the gold nanoparticle surface. Owing to the very small size, the nanoparticles contain a very high fraction of surface atoms, which, unlike the bulk atoms, have dangling valences. Apparently, this endows the surface with special electromagnetic properties. Presumably, as opposed to the bulk metal, which is diamagnetic, gold nanoparticles behave as ferromagnets at low temperature and form a magnetic field, which induces the spin flip in protium nuclei. Gold nanoparticles indeed exhibit ferromagnetism not inherent in the bulk material [37]. According to the data of the study cited, the external magnetic field and temperature dependence of the ESM signal suggests that magnetization of Au nanoparticles consists of a superparamagnetic part obeying the Curie law and a temperature-independent Pauli-paramagnetic part. The mixture of these components is reasonably explained by the picture that the surface atoms are ferromagnetic and the bulk atoms are Pauli-paramagnetic. Indeed, in a number of publications, the presence of ferromagnetic properties in nanosized gold particles was detected experimentally [38]. Previously, it was demonstrated [5] that hydrogen adsorption of gold nanoparticles induces a shift of the optical band for surface plasmon resonance to shorter wavelengths. This attests to increase in the electron density on gold particles as a result of hydrogen adsorption. Apparently, the weak coupling between the hydrogen and the gold surface is a prerequisite for the observation of spin polarization. Presumably, ortho-para hydrogen conversion is rate-limited by the hydrogen adsorption-desorption on gold nanoparticles.

#### 4. CONCLUSION

It is exhibited that all Au/ $\gamma$ -AL<sub>2</sub>O<sub>3</sub> catalyst with nanoparticles of 4.6-40.1 nm sizes show very high catalytic activity in *ortho-para* conversion reaction. The calculated specific catalytic activity  $K_{sp}$  of *ortho-para* hydrogen conversion were  $(3.9 \pm 1.2) \times 10^{14}$  molecules / (cm<sup>2</sup>·s) for all of the catalysts tested. The conversion of *o*-protium to *p*-protium catalyzed by gold nanoparticles does not depend on the nanoparticle size.

#### ACKNOWLEDGEMENTS

***This work was partly supported (B.G.E., E.V.A., R.D.S.) by the Russian Foundation for Basic Research under Grant number 15-03-02068-a.***

#### REFERENCES

- [1] HARUTA M. Size- and support-dependency in the catalysis of gold. *Catal. Today*, 1997, vol. 36, pp. 153-166.
- [2] BOND, G. C, THOMPSON, D. T. Catalysis by Gold. *Catal. Rev.: Sci. Eng.*, 1999, vol. 41, pp. 319-388.
- [3] SCHIMPF, S, LUCAS, M., MOHR, C., RODEMERCK, U., BRÜCKNER, A., RADNIK, J., HOFMEISTER, H., CLAUS, P. Supported gold nanoparticles: in-depth catalyst characterization and application in hydrogenation and oxidation reactions. *Catal. Today*, 2002, vol. 72, pp. 63-78.
- [4] JAWALE, D. V., GRAVEL, E., GEERTSEN, V., LI, H., SHAH, N., KUMAR, R., JOHN, J., NAMBOOTHIRI, I. N. N., DORIS, E. Size effect of gold nanoparticles supported on carbon nanotube as catalysts in selected organic reactions. *Tetrahedron*, 2014, vol. 70 pp. 6140-6145.
- [5] ERSHOV, B. G., ABKHALIMOV, E. V., SOLOVOV, R. D., ROLDUGHIN, V. I. Gold nanoparticles in aqueous solutions: influence of size and pH on hydrogen dissociative adsorption and Au(III) ion reduction. *Phys. Chem. Chem. Phys.*, 2016, vol. 18, pp. 13459-13466.
- [6] HERVÉS, P., PÉREZ-LORENZO, M., LIZ-MARZÁN, L. M., DZUBIELLA, J., LUBC, Y., BALLAUFF, M. Catalysis by metallic nanoparticles in aqueous solution: model reactions. *Chem. Soc. Rev.*, 2012, vol. 41, pp. 5577-5587.
- [7] DERAEDT, C., SALMON, L., GATARD, S., CIGANDA, R., HERNANDEZ, R., RUIZ, J., ASTRUC, D. Sodium borohydride stabilizes very active gold nanoparticle catalysts. *Chem. Commun.*, 2014, vol. 50, pp. 14194-14196.
- [8] LIN, C., TAO, K., HUA, D., MA, Z., ZHOU, S. Size Effect of Gold Nanoparticles in Catalytic Reduction of *p*-Nitrophenol with NaBH<sub>4</sub>. *Molecules*. 2013, vol. 18, pp. 12609-12620.
- [9] DEMIREL-GÜLEN, S., LUCAS, M., CLAUS, P. Liquid phase oxidation of glycerol over carbon supported gold catalysts. *Catal. Today*, 2005 vol. 102-103, pp. 166-172.

- [10] QIAN, K., LUO, L., BAO, H., HUA, Q., JIANGA, Z., HUANG, W. Catalytically active structures of SiO<sub>2</sub>-supported Au nanoparticles in low-temperature CO oxidation. *Catal. Sci. Technol.*, 2013, vol. 3, pp. 679-687.
- [11] VAN HARDEVELD, R., HARTOG, F. The statistics of surface atoms and surface sites on metal crystals. *Surf. Sci.*, 1969, vol. 15, pp. 189-230.
- [12] BOEVA, O. A., ERSHOV, B. G., ZHAVORONKOVA, K. N., ODINTSOV, A. A., SOLOVOV, R. D., ABKHALIMOV, E. V., EVDOKIMENKO, N. D. Catalytic properties of gold nanoparticles in H<sub>2</sub>-D<sub>2</sub> exchange and ortho-para hydrogen conversion. *Dokl. Phys. Chem.*, 2015, vol. 463, pp. 165-167.
- [13] FUKUTANI, K., SUGIMOTO, T. Physisorption and ortho-para conversion of molecular hydrogen on solid surfaces. *Prog. Surf. Sci.*, 2013, vol. 88, pp. 279-348.
- [14] ILISCA, E. Theory of the vibrational line shape of an adatom at a bridge site. *Prog. Surf. Sci.*, 1992, vol. 41, pp. 217-335.
- [15] SANDLER, Y. L., DURIGON, D. D. Low-temperature ortho-para conversion of hydrogen on silver. *Trans. Faraday Soc.*, 1966, vol. 62, pp. 15-221.
- [16] AVOURIS, P., SCHMEISSER, D., DEMUTH, J. E. Observation of Rotational Excitations of H<sub>2</sub> Adsorbed on Ag Surfaces. *Phys. Rev. Lett.*, 1982, vol. 48, pp. 199-202.
- [17] ILISCA, E. Ortho-para H<sub>2</sub> conversion on a cold Ag(111) metal surface. *Phys. Rev. Lett.*, 1991, vol. 66, pp. 667-670.
- [18] NIKI, K., KAWAUCHI, T., MATSUMOTO, M., FUKUTANI, K., OKANO, T. Mechanism of the ortho-para conversion of hydrogen on Ag surfaces. *Phys. Rev. B*, 2008, vol. 77, pp. 201404(R).
- [19] FUKUTANI, K., YOSHIDA, K., WILDE, M., DIÑO, W. A., MATSUMOTO, M., OKANO, T. Photostimulated Desorption and Ortho-Para Conversion of H<sub>2</sub> on Ag Surfaces. *Phys. Rev. Lett.*, 2003, vol. 90, pp. 096103.
- [20] ANDERSSON, S., HARRIS, J. Observation of Rotational Transitions for H<sub>2</sub>, D<sub>2</sub>, and HD Adsorbed on Cu(100). *Phys. Rev. Lett.*, 1982, vol. 48, pp. 545-548.
- [21] SVENSSON, K., ANDERSSON, S. Fast Ortho-Para Conversion of H<sub>2</sub> Adsorbed at Copper Surface Step Atoms. *Phys. Rev. Lett.*, 2007, vol. 98, pp. 096105.
- [22] PALMER, R. E., WILLIS, R. F. Rotational states of physisorbed hydrogen on graphite. *Surf. Sci.*, 1987, vol. 179, pp. L1-L5.
- [23] YUCEL, S., ALEXANDER, N., HONIG, A. Low-temperature catalysis of para-deuterium to ortho-deuterium conversion on Grafoil. *Phys. Rev. B*, 1990, vol. 42, pp. 820-825.
- [24] KIM, J. H., KARNG, S. W., OH, I. H., NAH, I. W. Ortho-para hydrogen conversion characteristics of amorphous and mesoporous Cr<sub>2</sub>O<sub>3</sub> powders at a temperature of 77 K. *Int. J. Hydrog. Energy*, 2015, vol. 40, pp. 14147-14153.
- [25] DAS, T., KWEON, S. C., CHOI, J. G., KIM, S. Y., OH, I. H. Spin conversion of hydrogen over LaFeO<sub>3</sub>/Al<sub>2</sub>O<sub>3</sub> catalysts at low temperature: Synthesis, characterization and activity. *Int. J. Hydrog. Energy*, 2015, vol. 40, pp. 383-391.
- [26] DAS, T., NAH, I. W., CHOI, J. G., OH, I. H. Synthesis of iron oxide catalysts using various methods for the spin conversion of hydrogen. *Reac. Kinet. Mech. Cat.*, 2016, vol. 118, pp. 669-681.
- [27] HARTL, M., GILLIS, R. C., DAEMEN, L., OLDS, D. P., PAGE, K., CARLSON, S., CHENG, Y., HÜGLE, T., IVERSON, E. B., RAMIREZ-CUESTA, A. J., LEE, Y., MUHRER, G. Hydrogen adsorption on two catalysts for the ortho-to parahydrogen conversion: Cr-doped silica and ferric oxide gel. *Phys. Chem. Chem. Phys.*, 2016, vol. 18, pp. 17281-17293.
- [28] MINAEV, B. F., AGREN, H. Spin Catalysis of Ortho-Para Hydrogen Conversion. *J. Phys. Chem.*, 1995, vol. 99, pp. 8936-8940.
- [29] BUNTKOWSKY, G., WALASZEK, B., ADAMCZYK, A., XU, Y., LIMBACH, H. H., CHAUDRET, B. Mechanism of nuclear spin initiated *para*-H<sub>2</sub> to *ortho*-H<sub>2</sub> conversion. *Phys. Chem. Chem. Phys.*, 2006, vol. 8, pp. 1929-1935.
- [30] WAKAO, N., SMITH, J. M., SELWOOD, P. W. The low-temperature orthohydrogen conversion over supported oxides and metals. *J. Catal.*, 1962, vol. 1, pp. 62-73.
- [31] ASHMEAD, D., ELEY, D. D., RUDHAM, R. The catalytic activity of the rare earth oxides for parahydrogen conversion and hydrogen-deuterium equilibration. *J. Catal.*, 1964, vol. 3, pp. 280-288.
- [32] MAKOSHI, K., RAMI, M., ILISCA, E. Dipolar and contact-processes in H<sub>2</sub> o-p-conversion on ionic surfaces. *J. Phys.: Condens. Matter.*, 1993, vol. 5, pp. 7325-7342.

- [33] TURKEVICH, J., STEVENSON, P. C., HILLIER, J. A study of the nucleation and growth processes in the synthesis of colloidal gold. *Discuss. Faraday Soc.*, 1951, vol. 11, pp. 55-75.
- [34] SOLOVOV, R. D., ERSHOV, B. G. Preparation of palladium nanoparticles with desired sizes in aqueous solutions. *Colloid J.*, 2014, vol. 76, pp. 595-599.
- [35] AROMAL, S. A., PHILIP, D. Facile one-pot synthesis of gold nanoparticles using tannic acid and its application in catalysis. *Physica E*, 2012, vol. 44, pp. 1692-1696.
- [36] FARKAS, L. Über Para- und Orthowasserstoff. *Ergebnisse exakt. Naturw.*, 1933, vol. 12, pp. 163-218.
- [37] YAMAMOTO, Y., MIURA, T., TERANISHI, T., MIYAKE, M., HORI, H., SUZUKI, M., KAWAMURA, N., MIYAGAWA, H., NAKAMURA, T., KOBAYASHI, K. Direct Observation of Ferromagnetic Spin Polarization in Gold Nanoparticles. *Phys. Rev. Lett.*, 2004, vol. 93, pp. 116801.
- [38] NEALON, G. L., DONNIO, B., GREGET, R., KAPPLER, J. P., TERAZZI, E., GALLANI, J. L. Magnetism in gold nanoparticles. *Nanoscale*, 2012, vol. 4, pp. 5244-5258.